

High-efficiency blue and green LEDs grown on Si with 5 micrometer thick GaN buffer

Xinbo Zou, Ka Ming Wong, Wing Cheung Chong, Jun Ma, and Kei May Lau*

Department of Electronic and Computer Engineering, Hong Kong University of Science and Technology, 999077, Hong Kong

Received 12 September 2013, revised 18 November 2013, accepted 17 December 2013

Published online 17 February 2014

Keywords GaN, LEDs, blue, green, buffer

* Corresponding author: e-mail eekmlau@ust.hk, Phone: +852 2358 7049, Fax: +852 2358 1485

High-efficiency blue and green light-emitting diodes (LEDs) were grown on planar Si substrates using a 5 μm thick GaN buffer by metalorganic chemical vapor deposition (MOCVD). AlN/GaN superlattices (SLs)-based interlayers were inserted twice for stress balancing and dislocation reduction. Smooth surface and low dislocation density of $1 \times 10^9 \text{ cm}^{-2}$ were achieved. The light output power (LOP) of bare $300 \times 300 \mu\text{m}^2$ 447 nm-LEDs and

510 nm-LEDs on Si was measured to be 2.15 mW and 0.85 mW at 20 mA, respectively. At -15 V, leakage current of as low as 3 μA was achieved for 447 nm-LEDs while higher leakage current was measured for green LEDs. After Si substrate removal, the LOP of packaged 440 nm- and 500 nm-LEDs reached 8.50 mW and 4.85 mW at 20 mA, respectively.

© 2014 WILEY-VCH Verlag GmbH & Co. KGaA, Weinheim

1 Introduction

GaN-based blue and green (430 nm to 550 nm) light-emitting diodes (LEDs) are ideal candidates for applications such as indicators, traffic signage, white light generation, and so on due to their color purity and long lifetime [1, 2]. Compared with sapphire and SiC substrates for GaN epitaxial growth, Si substrates offer some unique features including large size availability at low cost, good thermal conductivity, and the possibility of integrating GaN and Si-based devices [3]. However, it is very challenging to grow high-quality crack-free GaN epilayer on Si due to the large lattice constant mismatch ($\sim 17\%$) and significant thermal expansion coefficient difference ($\sim 54\%$) [4].

To grow crack-free GaN on Si with low dislocation density, various techniques such as SiN_x *in-situ* masks [5], AlN/AlGaIn-based buffers or intermediate layers [6], and porous Si substrate [7] have been utilized. Thick GaN epilayer growth on Si has been demonstrated by inserting AlN-based interlayers (ILs) several times [8]. Device results of blue LEDs on Si have been reported using different GaN buffers [9], however, there are few publications reporting device results of fabricated green LEDs on Si [10, 11], especially those after light-absorptive Si substrate removal. This is because green LEDs on Si tend to suffer from large dislocation density in the GaN buffer on Si and

inferior internal quantum efficiency in the active regions induced by higher indium composition [12].

In this paper, we report the growth and fabrication of blue and green GaN-based LEDs on Si substrates using a 5 μm -thick GaN buffer scheme. AlN/GaN superlattices (SLs)-based ILs were used for strain balancing, providing compressive stress to prevent film cracks. In addition to presenting material characteristics, device results of blue and green LEDs before and after Si substrate removal are reported. Comparisons between blue and green LEDs are made in terms of electrical and optical properties.

2 Experimental

The blue and green LED samples with 5 μm -thick GaN buffers were grown on 2-inch planar Si (111) substrates by metalorganic chemical vapor deposition (MOCVD) in an AIXTRON 2000HT system. A cross-sectional scanning electron microscope (SEM) image and a schematic of the LED with a 5 μm buffer are shown in Fig. 1(a) and (b). The MOCVD growth process is as follows: the Si substrate was firstly annealed at 1150 $^\circ\text{C}$ in H_2 atmosphere to remove native oxide. Then a 30 nm-thick-AlN nucleation layer was deposited, followed by *in-situ* growth of SiN_x masks. After that, 1 μm -thick undoped GaN was grown using an ammonia flow modulation method for coalescence

and dislocation reduction [13]. Next, the first 8 pairs of 10nm/25nm-thick AlN/GaN SLS-based interlayer (IL) was inserted to introduce compressive stress. Subsequently, a 1.5 μm -thick undoped GaN and a second IL (same as the first IL) were grown. Finally, a full LED structure, consisting of a 2 μm n-GaN layer, 5 pairs of 2.5nm/10nm-thick InGaN/GaN multi quantum wells (MQWs) and a 200 nm p-GaN layer was deposited. The GaN epilayer before the MQWs was 5 μm thick in total with two ILs inserted. The MQWs were grown in a N_2 atmosphere. The temperature-controlled indium composition in the MQWs was designed to be 16% and 23% for 447 nm- and 510 nm-LEDs, respectively, while the well and barrier thickness was set as the same.

A reference blue LED sample (REF-LED) with a relatively thinner GaN buffer and one IL was also grown for comparison (Fig. 1(c)). For the REF-LED, after growing the first GaN buffer and the first IL, a LED structure consisting of 1.5 μm n-GaN, MQWs, and 200 nm p-GaN was deposited on top to finish the growth. The total epilayer thickness of the REF-LED was 3.1 μm . After the growth, all the LED samples were fabricated into $300 \times 300 \mu\text{m}^2$ square dies using Ag/ITO as a current spreading layer.

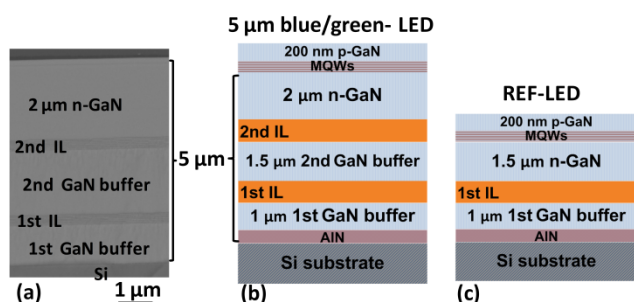


Figure 1 (a) Cross sectional SEM image of a LED sample grown on Si with a 5 μm buffer; (b,c) schematic diagrams of 5 μm blue/green-LEDs and REF-LED.

3 Results and discussion

Cross-sectional transmission electron microscopy (TEM) was used to investigate the dislocation evolution in the 5 μm GaN buffer, as shown in Fig. 2. The graph was made of three bright field images, all of which were collected near the GaN [1-100] zone axis so that all types of threading dislocations could be visible.

Threading dislocation (TD) density was reduced as GaN got coalesced over the *in-situ* SiN_x masks in the first GaN buffer, as previously reported [13]. In the second GaN buffer at least three types of TDs can be observed, which are labelled in Fig. 2: (I) a dislocation line bends and reacts with a neighbouring one, forming a half-loop or merging into one dislocation line; (II) TDs keep threading in the second GaN layer but got filtered by the second IL; and (III) TDs develop along the second GaN and thread through the above the second IL and the 2 μm n-GaN.

At the upper area of the second GaN buffer, the TD density was calculated to be $(5 \pm 1) \times 10^9 \text{ cm}^{-2}$, which represented the crystalline quality of the REF-LED because in the REF-LED, the MQWs were grown on top of the Si-doped second GaN layer. Whereas in the 5 μm -LEDs, a large number of TDs were stopped by the second IL (Type II), leading to a significantly reduced dislocation density at the upper region of the 2 μm n-GaN layer, $\sim (1 \pm 0.2) \times 10^9 \text{ cm}^{-2}$.

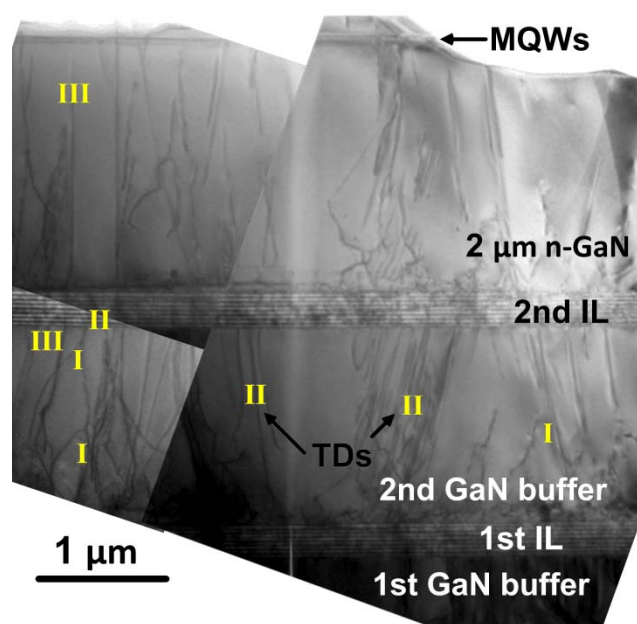
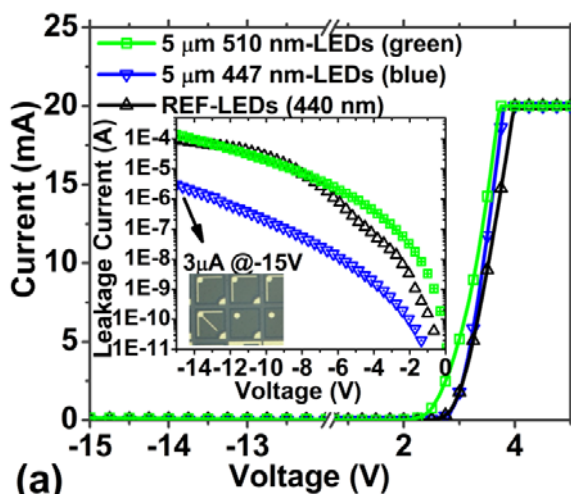


Figure 2 Composite TEM image showing TDs in the 5 μm GaN buffer.

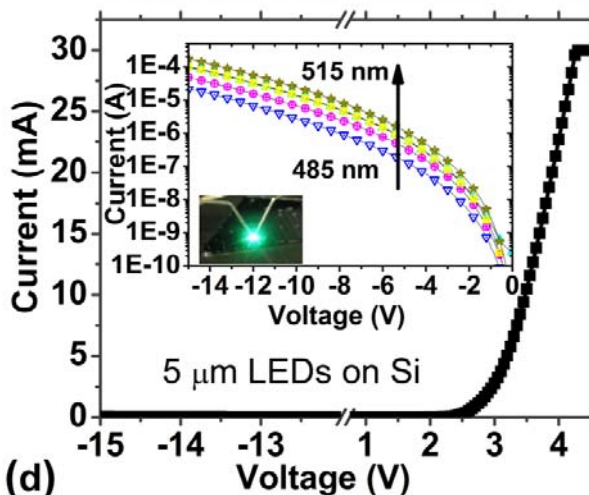
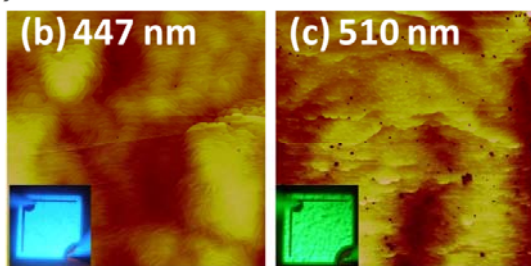
Figure 3(a) shows the current-voltage (I-V) characteristics of three fabricated LEDs on Si. With an injection current of 20 mA, the forward voltages were 3.95 V, 3.80 V, and 3.75 V for the REF-LED, 447 nm-LED (blue), and 510 nm-LED (green), respectively. The corresponding series resistances near 20 mA were calculated to be 45.5 Ω , 35.5 Ω , and 37.5 Ω , respectively. Compared with the REF-LED, the reduction of forward voltages and series resistance in both 5 μm -LEDs was related to the increase of n-GaN thickness from 1.5 μm to 2 μm , which facilitates current spreading in the n-GaN layers [14]. It also should be noted that the threshold voltage (V_{th}) of 510 nm-LED was around 2.4 V, which was 0.3 V lower than that in 447 nm-LED due to higher indium fraction in the green LEDs. Thus, at 20 mA, the forward voltage was still slightly lower for 510 nm-LED in spite of its relatively higher series resistance.

At reverse biases of -15 V and -5 V, the leakage currents of the 447 nm-LEDs were measured to be as low as 3.0 μA and 4.9 nA, both of which were more than one order lower compared with 93 μA and 220 nA in the REF-LED. Considering the similar indium fraction and emission wavelength in these two blue LEDs, the significantly re-

duced leakage current was attributed to the suppression of TDs-related leakage current paths in the 5 μm 447 nm-LEDs.



(a)



(d)

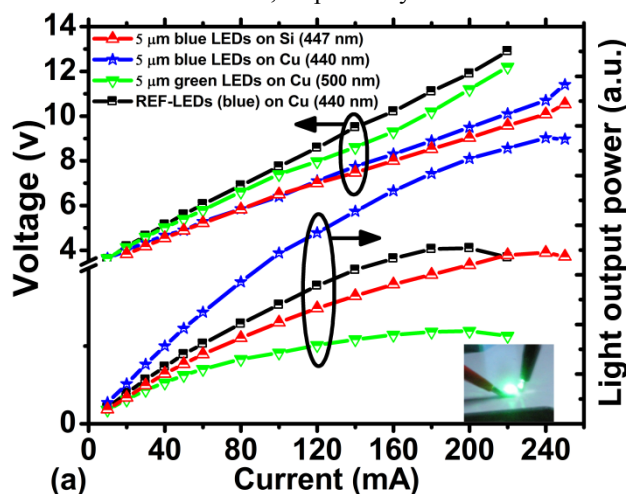
Figure 3 (a) I-V characteristics of 447nm-LEDs, 510 nm-LEDs, and REF-LEDs; (b, c) $10 \times 10 \mu\text{m}^2$ AFM scan of 447 nm- and 510 nm-LEDs; (d) dependence of leakage current on wavelength.

The measured leakage currents of 510 nm-LEDs were 140 μA and 1 μA at -15 V and -5 V, respectively, which were also higher than that of the 447 nm-LEDs. A comparison of the two LEDs' $10 \times 10 \mu\text{m}^2$ atomic force microscope (AFM) images revealed that the low density pits in the green LEDs could be the reason of higher leakage current, as shown in Fig. 3 (b) and (c). The surface of the 447

nm-LEDs is essentially featureless in term of surface defects whereas the 510 nm-LED presents a number of tiny pits, which are thought to be caused by the intersection of microscopic surfaces with dislocations.

Figure 3(d) illustrated the measured current-voltage (I-V) characteristics of the 5 μm -LEDs with wavelengths in the range from 485 nm to 515 nm. At -15 V, the leakage current steadily increased from 21 μA to 177 μA with increasing wavelength. Since the same 5 μm buffer scheme was used, the continuously increased indium composition and degraded InGaN crystalline quality in the longer wavelength-LEDs lead to larger leakage current.

In the electroluminescence (EL) measurement, the light output power (LOP) was measured in an integrating sphere using continuous-wave (CW) operation. At 20 mA injection current, the measured LOP of bare $300 \times 300 \mu\text{m}^2$ 447 nm-LEDs on Si was 2.15 mW, which was 45% higher than that of the REF-LED. The LOP improvement is attributed to the reduction of dislocation-related nonradiative centers and relief of current crowding effect. As the indium fraction was increased and wavelength red-shifted, the LOP dropped quickly. At 20 mA, LOP of 1.53 mW, 1.06 mW, and 0.85 mW was measured for 5 μm 485 nm-, 500 nm-, and 510 nm- LEDs on Si, respectively.



(a)

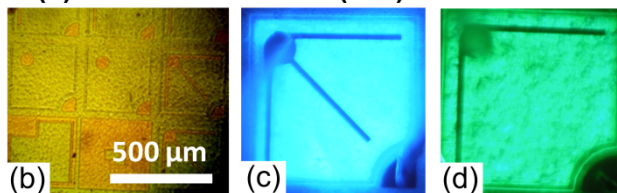


Figure 4 (a) L-I-V characteristics of the 5 μm blue-LEDs, 5 μm green-LEDs, and REF-LEDs encapsulated with silicone domes; (b) microscopic picture of LEDs transferred to Cu; (c, d) light-emitting images of $300 \times 300 \mu\text{m}^2$ 440 nm- and 500 nm-LEDs on Cu.

After preliminary characterization, the fabricated blue and green LEDs were transferred from Si to copper substrates by a Si removal process including insertion of a Ti/Al mirror layer. More process details can be found

elsewhere [15]. After transfer, both the blue and green LEDs on Cu showed higher forward voltage compared with corresponding LEDs on Si. There were two thermal process steps involved during transfer. One was polyimide solidification to protect front-side metal electrodes, while the other was silicone dome hardening. Both were done at a temperature of 150 degree Celsius for a few hours. The degradation of metal contact resistivity was believed to be the main reason for higher forward voltages in both blue and green LEDs [15]. Figure 4(a) shows the LOP-current-voltage (L-I-V) characteristics of packaged LEDs on Si and Cu substrates. For packaged 5 μm blue-LEDs, the measured LOP at 20 mA was 5.25 mW and 8.50 mW for 447 nm-LEDs on Si and 440 nm-LEDs on Cu, respectively. Compared with packaged REF-LEDs on Cu, which LOP saturated at 35.4 mW when driven with 200 mA, the 5 μm 440 nm-LEDs on Cu were saturated at a much higher level, 57.6 mW and 240 mA due to their higher internal quantum efficiency and less heat generation. For packaged 5 μm 500 nm-LEDs on Cu, as shown in Fig. 4(d), the measured LOP was 4.85 mW at 20 mA and the maximum LOP reached 18.7 mW at 200 mA.

4 Conclusions

In summary, we demonstrated high brightness GaN-based blue and green LEDs grown on Si substrates using a 5 μm thick GaN buffer scheme. The insertions of AlN/GaN SLs were not only effective in strain balancing but also filtered dislocations in the buffer. After Si removal and LED transfer, the optical power of packaged $300 \times 300 \mu\text{m}^2$ 440 nm- and 500 nm-LEDs were 8.50 mW and 4.85 mW at 20 mA, respectively. As a result of low leakage current and high internal quantum efficiency, the corresponding saturation LOP reached 57.6 mW at 240 mA and 18.7 mW at 200 mA, respectively.

Acknowledgements This work was supported in part by a grant (GHP/048/11) from the Innovation and Technology Commission (ITC), and a grant (T23-612/12-R) from the Research Grants Council of the Hong Kong Special Administrative Region Government under the Theme-based Research Scheme.

References

- [1] M. Peter, A. Laubsch, W. Bergbauer, T. Meyer, M. Sabathil, J. Baur, and B. Hahn, *Phys. Status Solidi A* **206**, 1125 (2009).
- [2] M. H. Crawford, *IEEE Sel. Top. Quantum Electron.* **15** 1028 (2009).
- [3] A. Dadgar, C. Hums, A. Diez, J. Blasing, and A. Krost, *J. Cryst. Growth* **297**, 279 (2006).
- [4] A. Dadgar, J. Blasing, A. Diez, A. Alam, M. Heuken, and A. Krost, *Jpn. J. Appl. Phys.* **39**(2), L1183-L5 (2000).
- [5] K. Cheng, M. Leys, S. Degroote, M. Germain, and G. Borghs, *Appl. Phys. Lett.* **92**, 192111 (2008).
- [6] E. Arslan, M. K. Ozturk, A. Teke, S. Ozcelik, and E. Ozbay, *J. Phys. D, Appl. Phys.* **41**, 155317 (2008).
- [7] D. M. Deng, C. H. Chiu, H. C. Kuo, P. Chen, and K. M. Lau, *J. Cryst. Growth* **315**, 238 (2011).
- [8] H. P. D. Schenk, E. Frayssinet, A. Bavard, D. Rondi, Y. Cordier, and M. Kennard, *J. Cryst. Growth* **314**, 85 (2011).
- [9] A. Dadgar, C. Hums, A. Diez, F. Schulze, J. Blasing, and A. Krost, *Advanced LEDs for Solid State Lighting*, edited by C. H. Hong et al. (2006), pp. U85-U92.
- [10] C. F. Shih, N. C. Chen, C. A. Chang, and K. S. Liu, *Jpn. J. Appl. Phys.* **44**(2), L140-L3 (2005).
- [11] T. Egawa and B. A. B. A. Shuhaimi, *J. Phys. D, Appl. Phys.* **43**, 354008 (2010).
- [12] Y. Li, S. You, M. Zhu, L. Zhao, W. Hou, T. Detchprohm, Y. Taniguchi, N. Tamura, S. Tanaka, and C. Wetzel, *Appl. Phys. Lett.* **98**, 151102 (2011).
- [13] X. Zou, K. M. Wong, N. Yu, P. Chen, and K. M. Lau, *Phys. Status Solidi C* **9**, 572 (2012).
- [14] X. Guo and E. F. Schubert, *J. Appl. Phys.* **90**, 4191 (2001).
- [15] K. M. Wong, X. Zou, P. Chen, and K. M. Lau, *IEEE Electron Device Lett.* **31**, 132 (2010).